Towards Realistic Transfer Rates within the Coupled Molecular Dynamics/Lattice Monte Carlo Approach

Supporting Information

Gabriel Kabbe, Christian Dreßler, and Daniel Sebastiani*

Institute of Chemistry, Martin-Luther-University Halle-Wittenberg, von-Danckelmann-Platz 4, 06120 Halle, Germany

E-mail: daniel.sebastiani@chemie.uni-halle.de

Lifetime of a $P(OH)_3$ Group

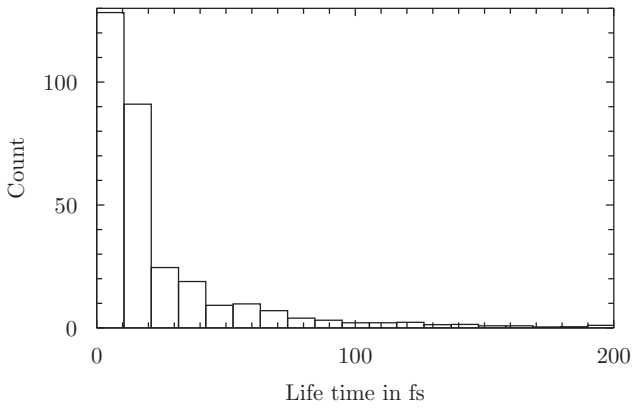

Figure 1: Lifetime of a $P(OH)_3$ group of 6(*p*-phosphonatophenyl)benzene in fs.

Activation Energy Functions of a CsH_2PO_4 Dimer and between $CsHSO_4$ and CsH_2PO_4

The uncertainty of the fit function of E_a^{PES} was determined via

$$u^{\mathrm{PES}}(d_{\mathrm{OO}}) = \sqrt{\left(\frac{\partial E_a^{\mathrm{PES}}}{\partial a}\Delta a\right)^2 + \left(\frac{\partial E_a^{\mathrm{PES}}}{\partial b}\Delta b\right)^2 + \left(\frac{\partial E_a^{\mathrm{PES}}}{\partial d_0}\Delta d_0\right)^2} \tag{1}$$

Its uncertainty owing to the uncertainties of the fit parameters is drawn as a blue dotted line.

Table 1: Fit parameters of the activation energy function $E_a(d)$ of a Sulfuric acid dimer

Parameter	Value	Unit
a	35 ± 2	kcal/mol/Å^2
b	0.2 ± 0.1	Å^{-2}
d_0	2.07 ± 0.02	Å

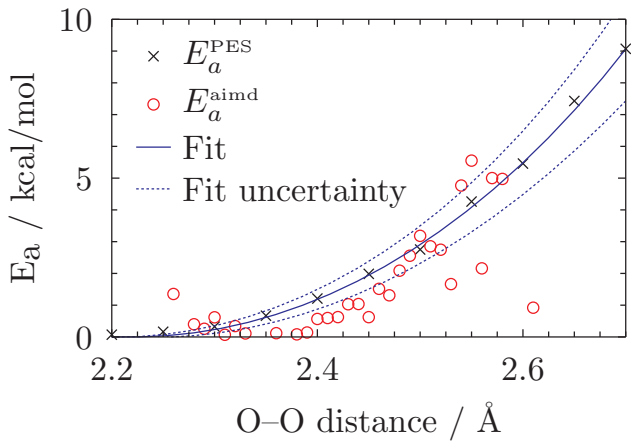

Figure 2: Fit of the activation energy of a proton jump over the oxygen distance in the phosphoric acid dimer

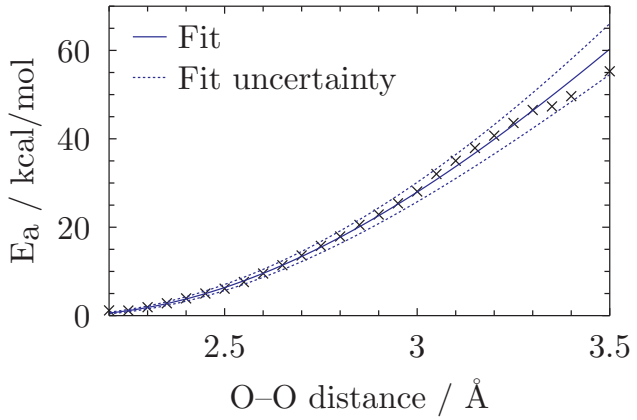

Figure 3: Fit of the activation energy of a proton jump over the oxygen distance in the sulfuric acid dimer

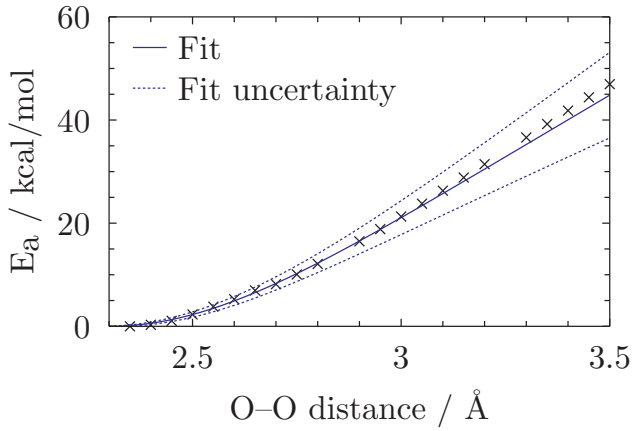

Figure 4: Fit of the activation energy of a proton jump over the oxygen distance between a phosphoric acid monomer and a sulforic acid monomer.

Table 2: Fit parameters of the activation energy function $E_a(d)$ between Sulfuric and Phosphoric acid

Parameter	Value	Unit
a	59 ± 7	kcal/mol/Å^2
b	1.8 ± 0.7	Å^{-2}
d_0	2.30 ± 0.02	Å

Comparison of a Proton Transfer Surface Scan in CsH_2PO_4 with and without Excess Protons

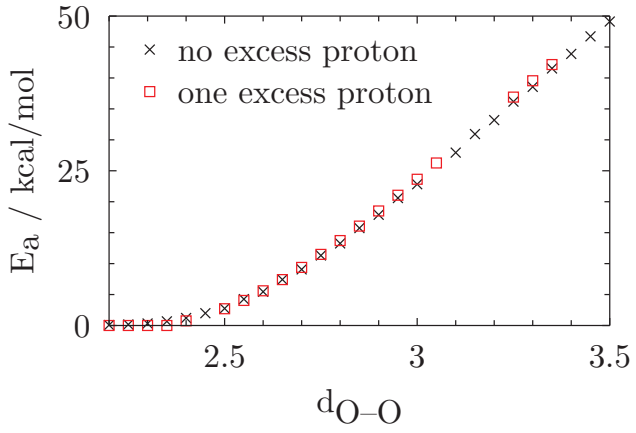

Figure 5: Comparison of the resulting activation energies of the Phosphoric acid dimer in the case of a neutral system (crosses), and with an additional proton (boxes).

Determination of Proton Jump Rates from AIMD

This method counts the number of proton jumps in an AIMD trajectory occurring between oxygen pairs at different distances. The script we use iterates over the whole trajectory, calculating for time t a histogram of distances between all singly occupied oxygen pairs $N_{\text{pairs}}(d_{\text{O–O}})$ (singly occupied means, that one oxygen is bonded covalently to a proton whereas the other one is not), and then checking at time $t + \Delta t$, between how many of those pairs a jump occurred, calling the resulting number $N_{\text{jumps}}(d_{\text{O–O}})$. A jump is defined here as the event, where the closest oxygen neighbor of a proton changes. This way, for

each oxygen distance in the histogram, a ratio $\frac{N_{\text{jumps}}(t+\Delta t, d_{\text{O–O}})}{N_{\text{pairs}}(t, d_{\text{O–O}})}$ is obtained. We calculate the distance-dependent jump rate then by averaging this ratio over all times in the trajectory.

$$\omega^{\text{aimd}}(d_{\text{O–O}}) \approx \frac{1}{\Delta t} \left\langle \frac{N_{\text{jumps}}\left(t + \Delta t, d_{\text{O–O}}\right)}{N_{\text{pairs}}\left(t, d_{\text{O–O}}\right)} \right\rangle_t \tag{2}$$

However, there are two aspects that led us to choose the Arrhenius approach rather than the above alternative. Firstly, the Arrhenius scheme provides more chemical insight into the protonation dynamics mechanism. Secondly, the trajectory analysis was found to require extensive statistics, corresponding to long AIMD runs, which are computationally resource intense.

The distance dependency of the jump rate constitutes the main influence of the molecular geometry on the proton jump rate. However, previous studies indicated that additional parameters are necessary in order to improve the agreement between LMC and AIMD.

Jump Rates Determined from AIMD and Jump Rates from the New Arrhenius Method in Comparison

The uncertainty of ω^{PES} is calculated analogously to equation 1.

6(*p*-phosphonatophenyl)benzene

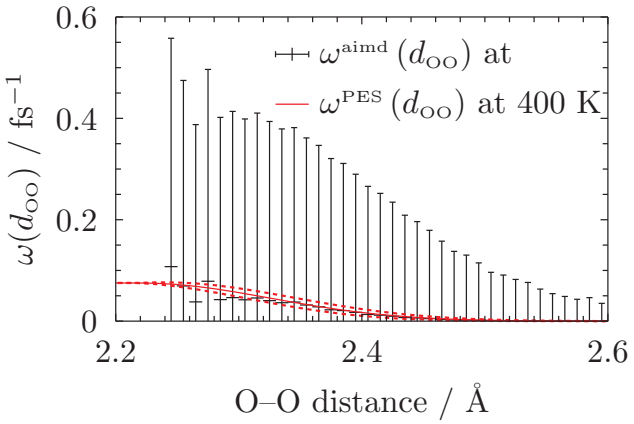

Figure 6: Comparison of jump rates in p- PA-HPB at 400 K. ω^{PES} with uncertainty (red dotted lines) and ω^{aimd} with statistical error (black error bars).

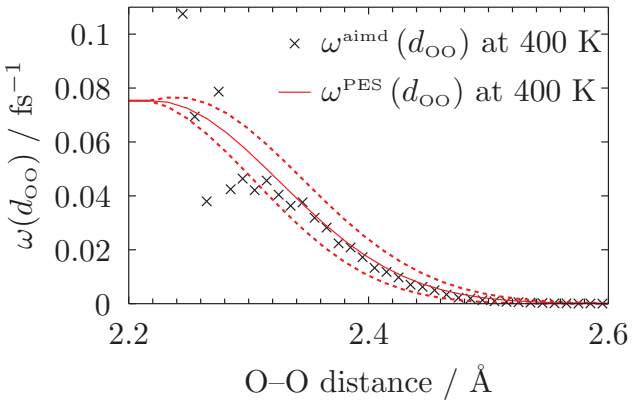

Figure 7: Comparison of jump rates in p- PA-HPB at 400 K. ω^{PES} with uncertainty (red dotted lines).

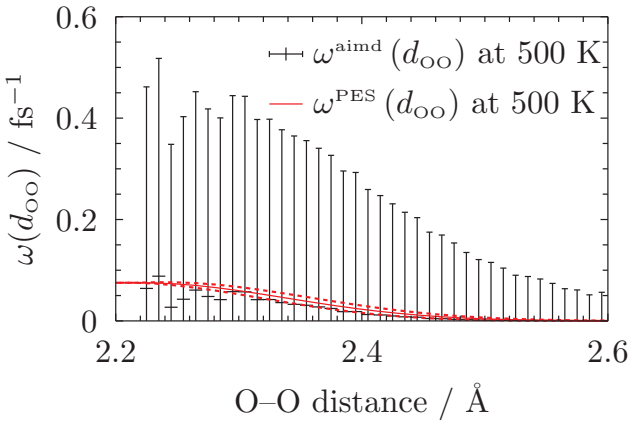

Figure 8: Comparison of jump rates in p- PA-HPB at 500 K. ω^{PES} with uncertainty (red dotted lines) and ω^{aimd} with statistical error (black error bars).

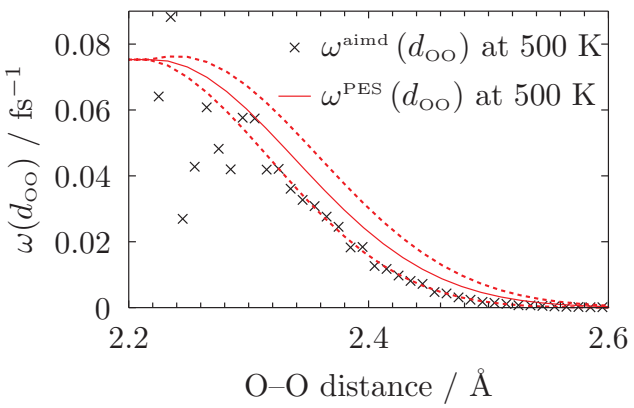

Figure 9: Comparison of jump rates in p- PA-HPB at 500 K. ω^{PES} with uncertainty (red dotted lines).

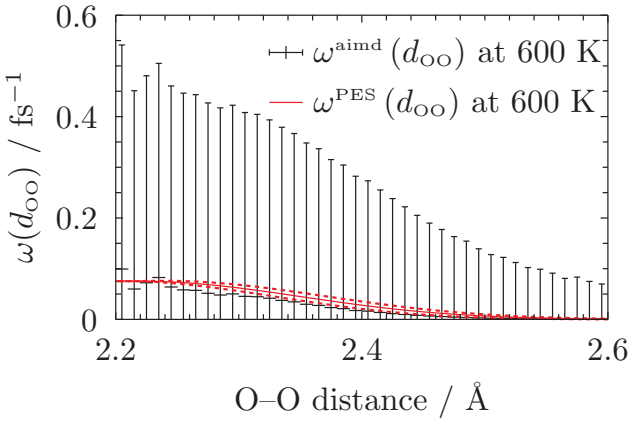

Figure 10: Comparison of jump rates in p- PA-HPB at 600 K. ω^{PES} with uncertainty (red dotted lines) and ω^{aimd} with statistical error (black error bars).

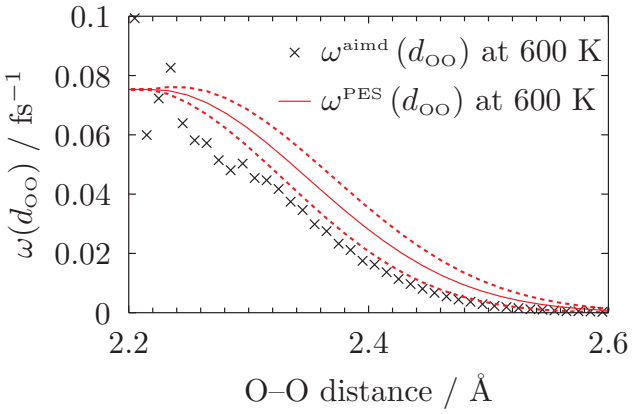

Figure 11: Comparison of jump rates in p- PA-HPB at 600 K. ω^{PES} with uncertainty (red dotted lines).

CsH_2PO_4

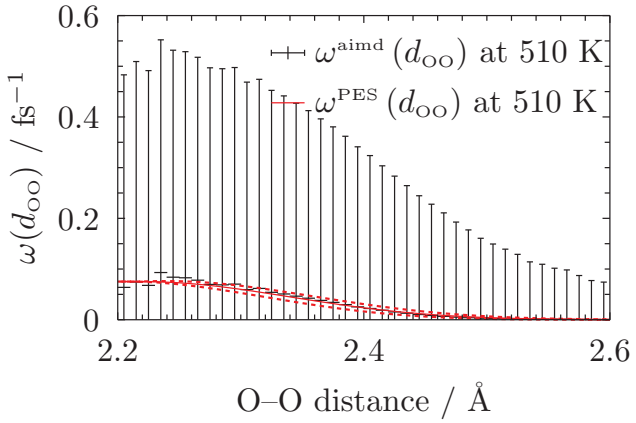

Figure 12: Comparison of jump rates in CsH_2PO_4 at 510 K. ω^{PES} with uncertainty (red dotted lines) and ω^{aimd} with statistical error (black error bars).

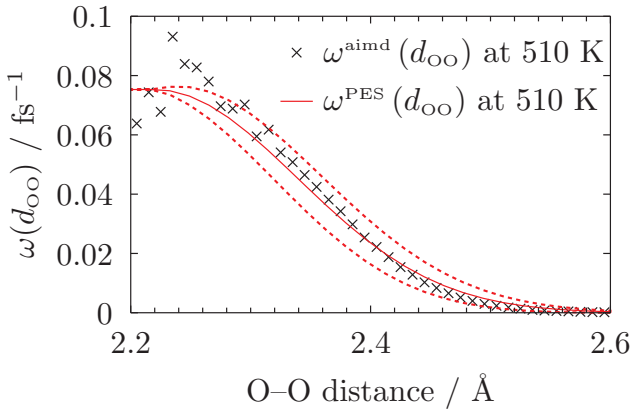

Figure 13: Comparison of jump rates in CsH_2PO_4 at 510 K. ω^{PES} with uncertainty (red dotted lines).

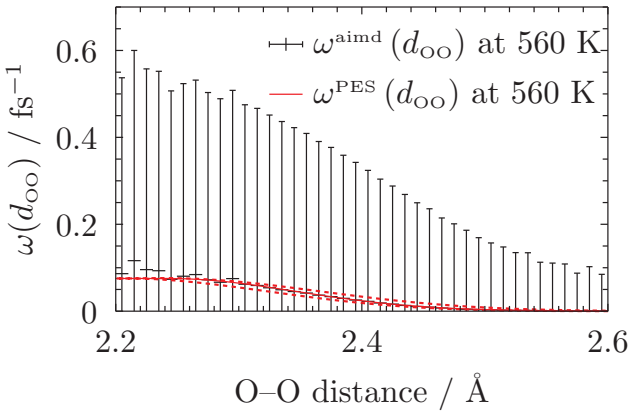

Figure 14: Comparison of jump rates in CsH_2PO_4 at 560 K. ω^{PES} with uncertainty (red dotted lines) and ω^{aimd} with statistical error (black error bars).

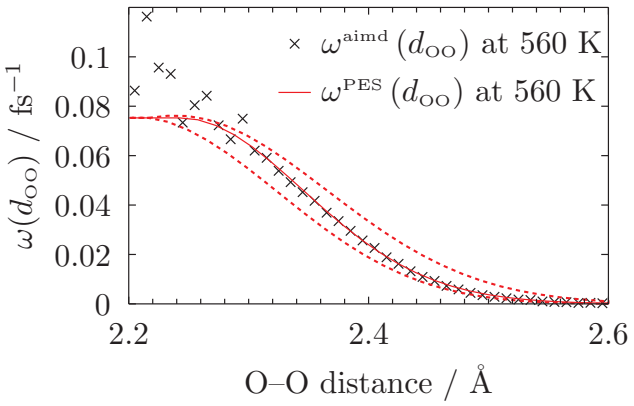

Figure 15: Comparison of jump rates in CsH_2PO_4 at 560 K. ω^{PES} with uncertainty (red dotted lines).

Free Energy Calculation from $E_a^{\mathbf{PES}}(d_{\mathbf{OO}})$

In order to confirm the validity of the previously determined activation energy function, we determine the free energy barrier of a proton transfer using the free energy perturbation formula, which gives the free energy difference between two states $\mathcal{A}$ and $\mathcal{B}$:

$$\Delta F_{\mathcal{AB}} = -k_B T \ln \left\langle e^{U_{\mathcal{B}} - U_{\mathcal{A}}} \right\rangle_{\mathcal{A}} \tag{3}$$

As state $\mathcal{A}$ we define each hydrogen bond, where the proton resides close the energy minimum around 1.1 Å away from an oxygen atom. As state $\mathcal{B}$ we define each hydrogen bond, where the proton sits exactly in the middle between donor and acceptor. We express the energy difference between the two states *via* equation **??**.

$$\Delta F_{\mathcal{AB}} = -k_B T \ln \left\langle e^{-E_a^{\mathrm{PES}}(d_{\mathrm{OO}})} \right\rangle_{\mathcal{A}} \tag{4}$$

In combination with equation 4, we determine the free energy of a proton hop for CsH_2PO_4 at 510 K. We identified the hydrogen bonds (i.e. state $\mathcal{A}$) in the CsH_2PO_4 trajectory using a geometric criterion ($d_{\mathrm{OH}} \leq 1.2$ Å, $d_{\mathrm{O}\cdots\mathrm{H}} \leq 2.2$ Å, and 140 °$\leq \measuredangle\mathrm{OHO} \leq$ 180 °) and determined $e^{-E_a^{\mathrm{PES}}}$ whenever the hydrogen bond criterion was fulfilled. Evaluating equation 4 results in a free energy of 0.1 eV for a proton transfer, which is in agreement with previous *ab initio* molecular dynamics (AIMD) simulations.[1]

Angular Dependence of the Proton Jump Rate – Benchmarks

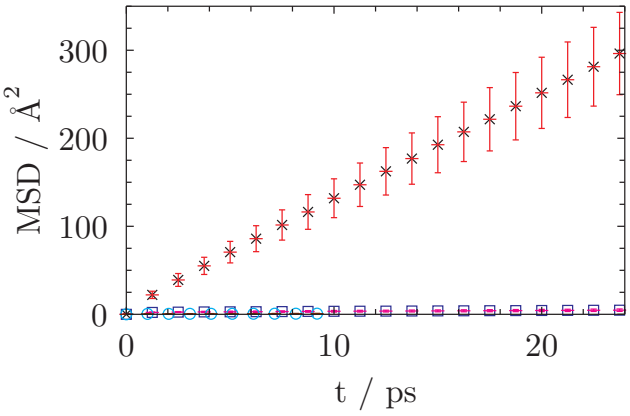

Figure 16: CsH_2PO_4 at 510 K

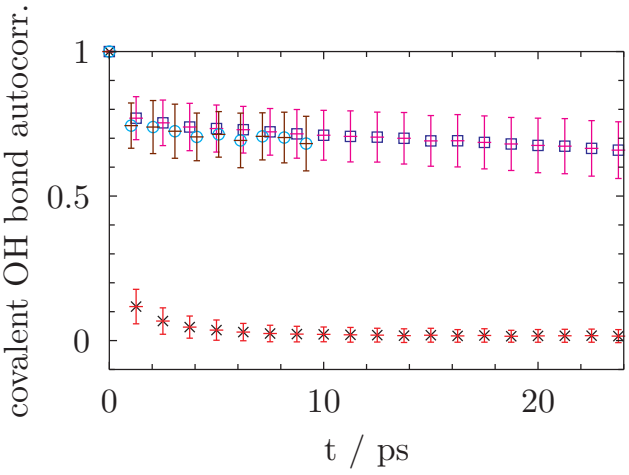

Figure 17: CsH_2PO_4 at 510 K

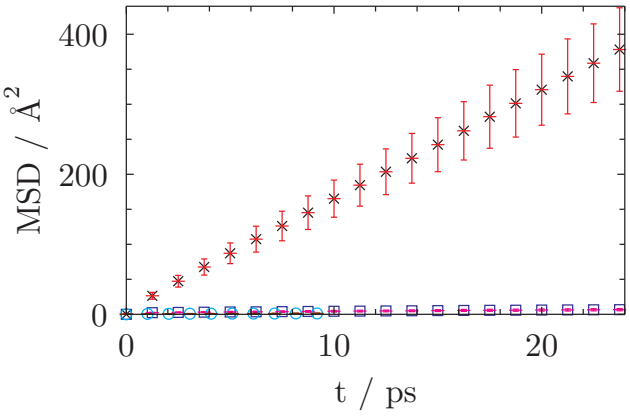

Figure 18: CsH_2PO_4 at 560 K

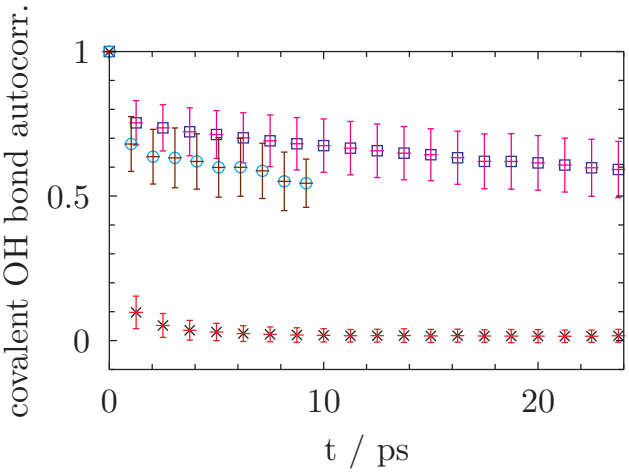

Figure 19: CsH_2PO_4 at 560 K

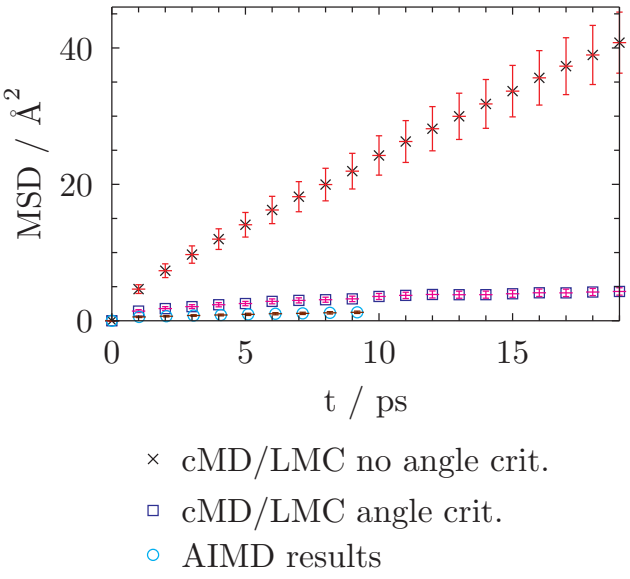

Figure 20: 6(*p*-phosphonatophenyl)benzene at 400 K

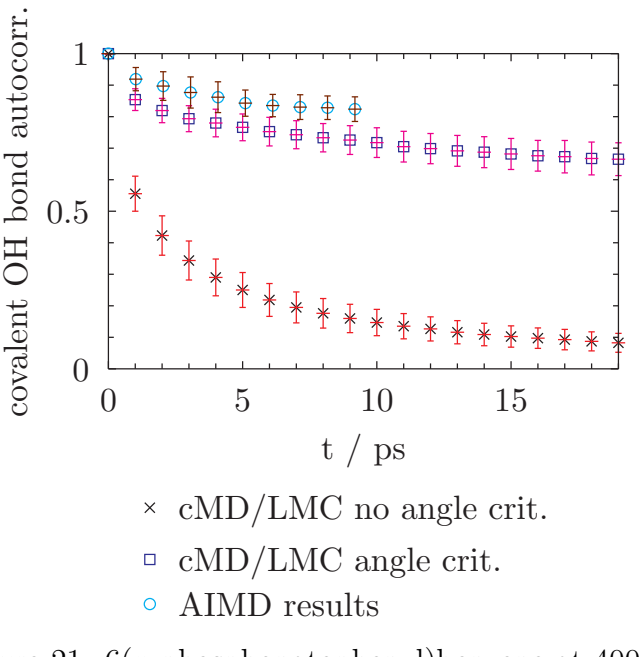

Figure 21: 6(*p*-phosphonatophenyl)benzene at 400 K

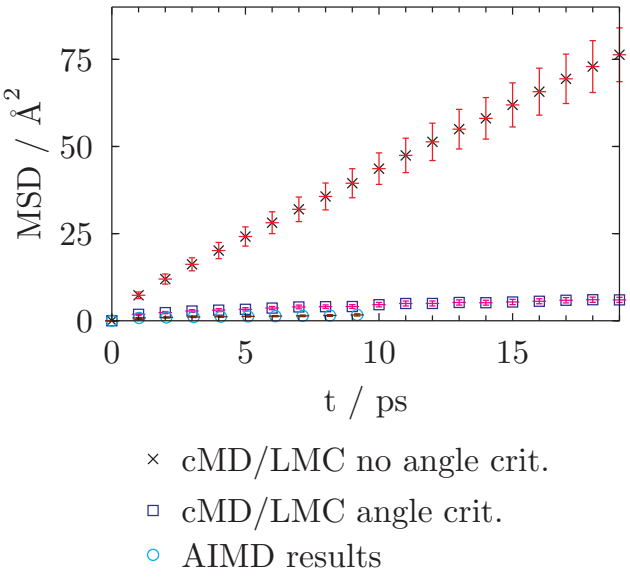

Figure 22: 6(*p*-phosphonatophenyl)benzene at 500 K

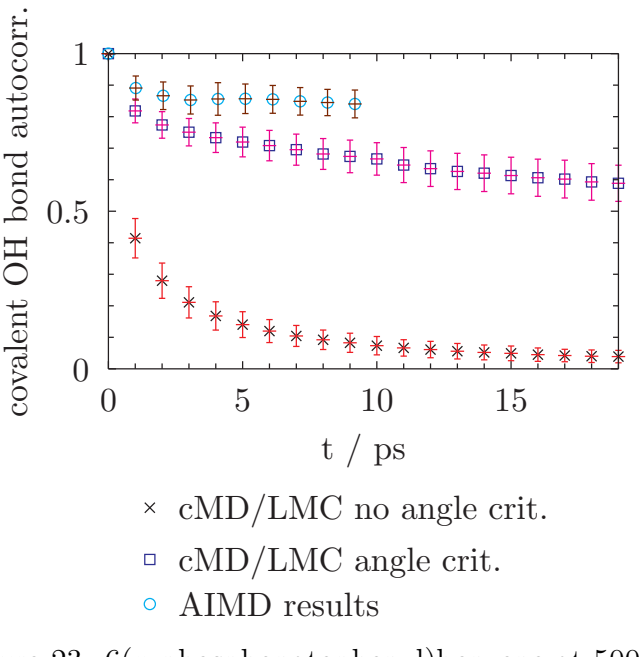

Figure 23: 6(*p*-phosphonatophenyl)benzene at 500 K

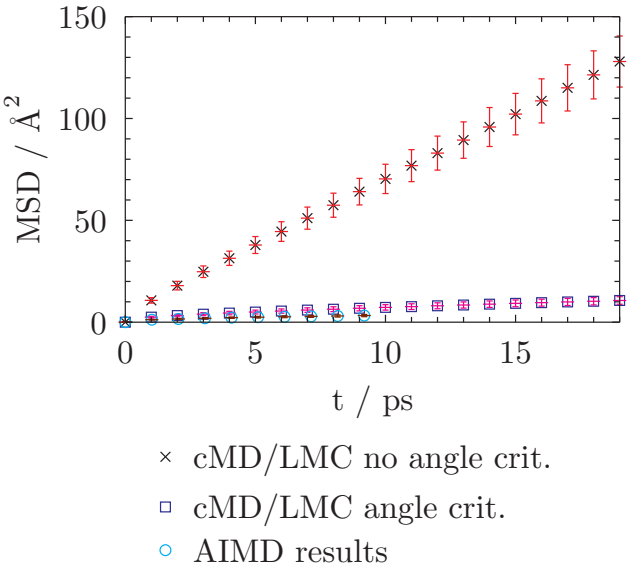

Figure 24: 6(*p*-phosphonatophenyl)benzene at 600 K

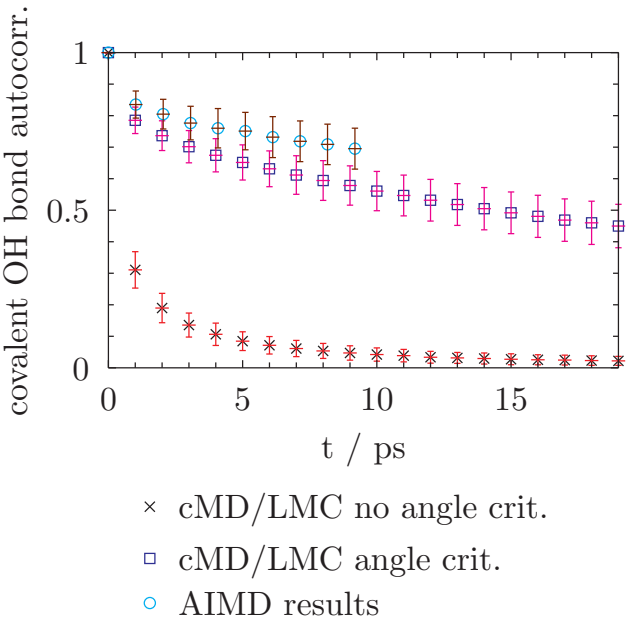

Figure 25: 6(*p*-phosphonatophenyl)benzene at 600 K

OH Vibration Frequencies

The OH vibration frequencies were determined as follows. For each AIMD trajectory and each acidic proton, we searched intervals with a length of 500 AIMD timesteps, in which the average OH distance was not larger than 1.1 Å, and the variance was below 0.0049 Å^2. We performed a Fourier transform on each interval and averaged the resulting frequency distributions.

Similarly, analyzing the OH vibration frequencies in the AIMD trajectories, we find a value for A between around 0.07 fs^{-1} and 0.1 fs^{-1} (considering the full width at half maximum (FWHM) of the main peaks found in the frequency distribution of p-6 PA-HPB in fig. 29).

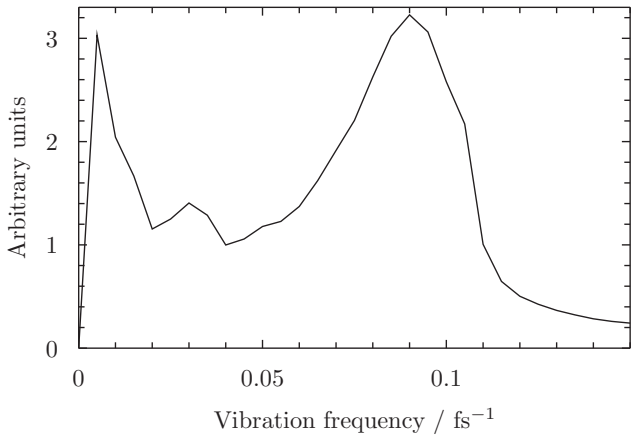

Figure 26: OH vibration frequencies of p-6 PA-HPB at 400 K.

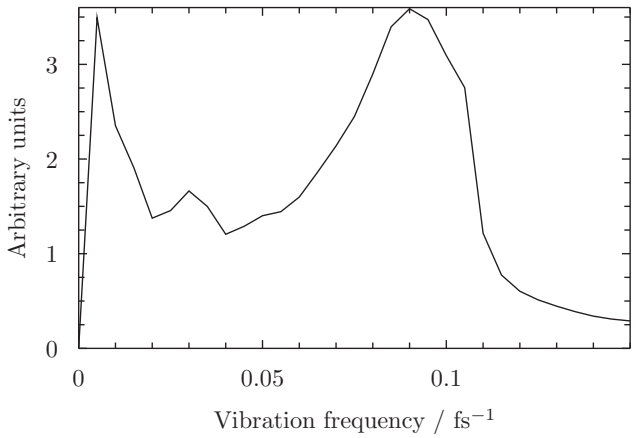

Figure 27: OH vibration frequencies of p-6 PA-HPB at 500 K.

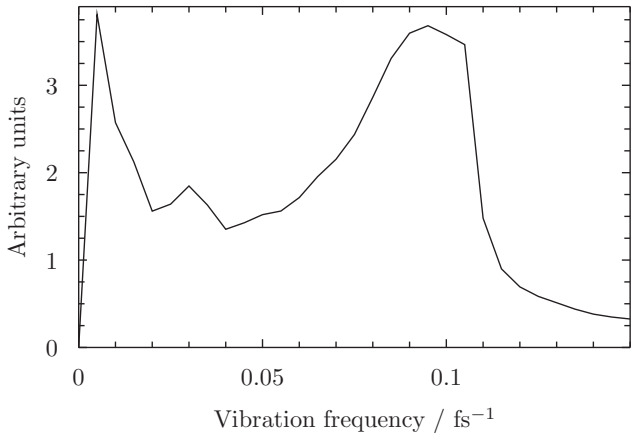

Figure 28: OH vibration frequencies of *p*-6 PA-HPB at 600 K.

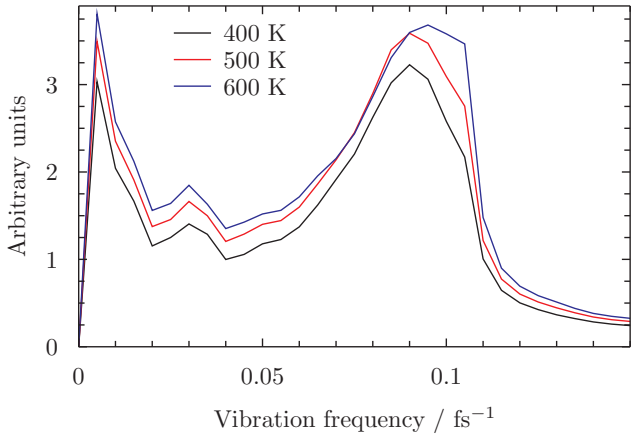

Figure 29: OH vibration frequencies of *p*-6 PA-HPB at 400, 500 and 600 K.

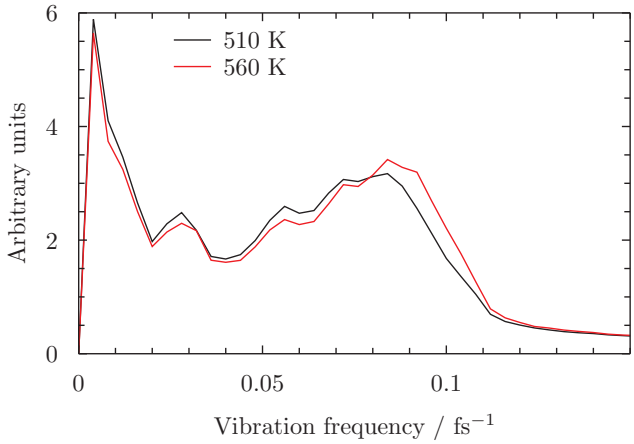

Figure 30: OH vibration frequencies of CsH_2PO_4 at 510 K.

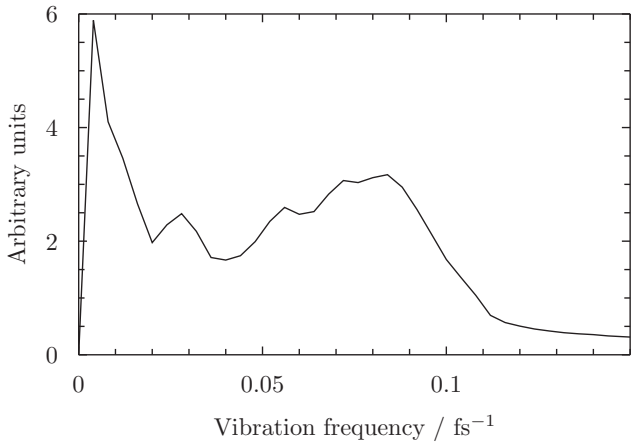

Figure 31: OH vibration frequencies of CsH_2PO_4 at 510 K.

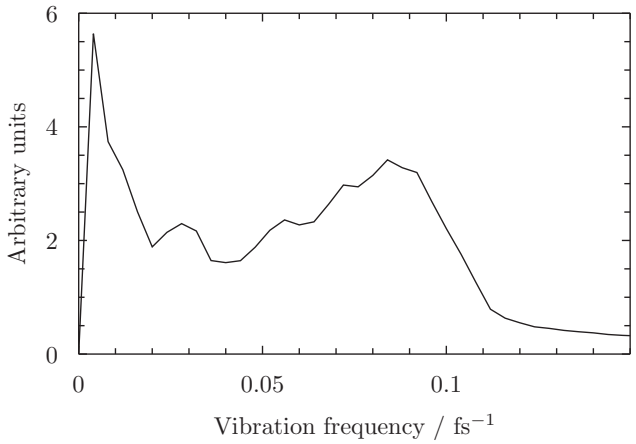

Figure 32: OH vibration frequencies of CsH_2PO_4 at 560 K.

Oxygen and Proton MSD over Trajectory Length

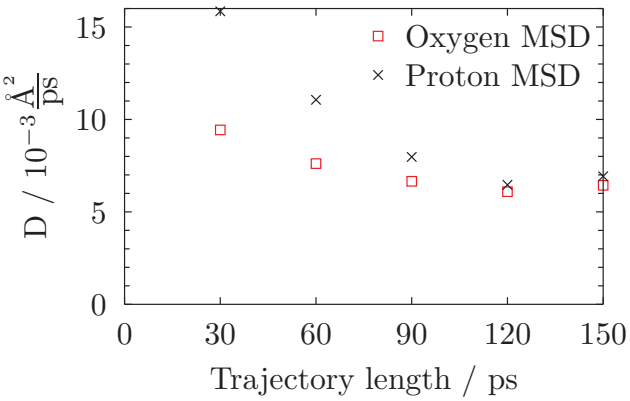

Figure 33: Oxygen MSD and proton MSD of CsH_2PO_4 at 510 K for trajectory lengths from 30 ps to 150 ps.

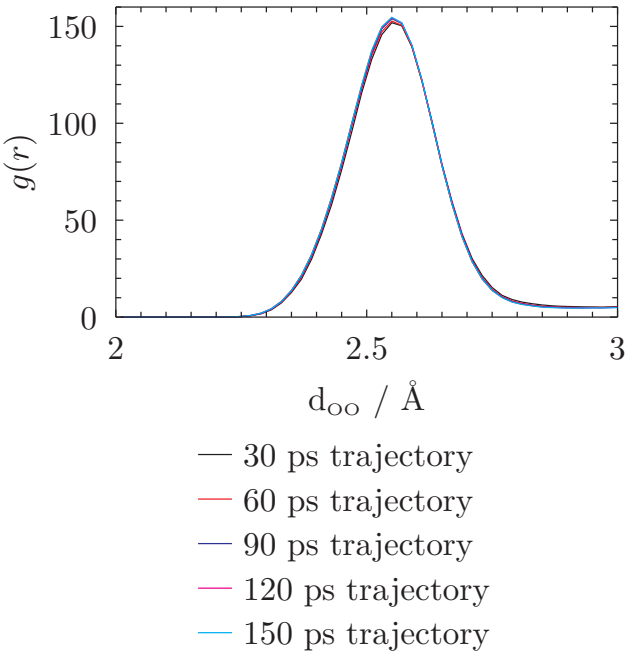

Figure 34: Oxygen radial distribution function of CsH_2PO_4 at 510 K for trajectory lengths from 30 ps to 150 ps.

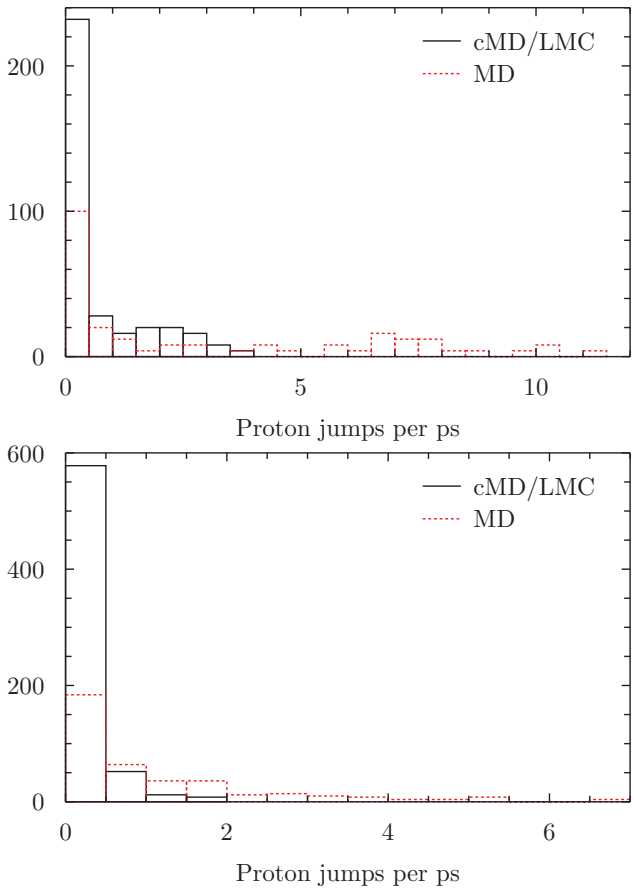

Figure 35: Histogram of the proton jump frequency between oxygen pairs in CsH_2PO_4 (left picture) and *p*-6 PA-HPB (right picture). For each oxygen pair, the number of proton jumps per ps was counted. Oxygen pairs which exhibited no proton jumps were not considered.

Comparison of the Proton Jump Frequency in MD and cMD/LMC

We compare the proton dynamics of the cMD/LMC model and the AIMD simulations by counting the number of proton jumps between every oxygen pair (O_i, O_j). We do this once for the protons in the AIMD, and once for the protons in the cMD/LMC model. Figure 35 shows the proton jump distribution of CsH_2PO_4 and *p*-6 PA-HPB. In both figures, the cMD/LMC model shows a considerably higher amount of oxygen pairs with a very low number of proton jumps. At the same time, oxygen pairs with a high number of proton jumps can only be found in the AIMD simulation.

The distribution of the proton jump frequencies in the cMD/LMC model shows that the cMD/LMC model does not yet satisfiably reproduce the proton dynamics of the AIMD. We think the reason for this is that the cMD/LMC model does not yet consider the protonation state of a phosphonic group when calculating the jump rates. Therefore, a jump from a $P(OH)_3$ group to a $PO(OH)_2$ group has the same probability as a jump between two $PO(OH)_2$ groups, even though the former would be energetically more favourable.

References

(1) Lee, H.-S.; Tuckerman, M. E. The Structure and Proton Transport Mechanisms in the Superprotonic Phase of CsH2PO4: An Ab Initio Molecular Dynamics Study. *J. Phys. Chem. C* **2008**, *112*, 9917–9930.